

# Pulsating fluid induced dynamic stability of embedded viscoelastic piezoelectric separators using different cylindrical shell theories

H. Rahimi Pour<sup>\*1</sup>, A. Ghorbanpour Arani<sup>1,2</sup> and G.A. Sheikhzadeh<sup>1</sup>

<sup>1</sup> Faculty of Mechanical Engineering, University of Kashan, Kashan, Iran

<sup>2</sup> Institute of Nanoscience & Nanotechnology, University of Kashan, Kashan, Iran

(Received March 16, 2017, Revised May 26, 2017, Accepted May 31, 2017)

**Abstract.** This paper deals with nonlinear dynamic stability of embedded piezoelectric nano-composite separators conveying pulsating fluid. For presenting a realistic model, the material properties of structure are assumed viscoelastic based on Kelvin-Voigt model. The separator is reinforced with single-walled carbon nanotubes (SWCNTs) which the equivalent material properties are obtained by mixture rule. The separator is surrounded by elastic medium modeled by nonlinear orthotropic visco Pasternak foundation. The separator is subjected to 3D electric and 2D magnetic fields. For mathematical modeling of structure, three theories of classical shell theory (CST), first order shear deformation theory (FSDT) and sinusoidal shear deformation theory (SSDT) are applied. The differential quadrature method (DQM) in conjunction with Bolotin method is employed for calculating the dynamic instability region (DIR). The detailed parametric study is conducted, focusing on the combined effects of the external voltage, magnetic field, visco-Pasternak foundation, structural damping and volume percent of SWCNTs on the dynamic instability of structure. The numerical results are validated with other published works as well as comparing results obtained by three theories. Numerical results indicate that the magnetic and electric fields as well as SWCNTs as reinforcer are very important in dynamic instability analysis of structure.

**Keywords:** piezoelectric separators; viscoelastic; SSDT; DQM; orthotropic viscoelastic medium

## 1. Introduction

Separators which can be used commonly in oil and gas industry are a pressure vessel for separating the fluids into their constituent components of oil, gas and water. The separators can be divided into horizontal, vertical, or spherical separators. Usually, the inlet fluid of separators is pulsating and the dynamic stability analysis of them is essential. However, in this paper, the separator is simulated with a cylindrical shell conveying pulsating fluid.

Mechanical analysis of cylindrical shells has been investigated by many authors. The mechanism of wind-induced ovaling vibrations of cylindrical shells was numerically investigated by Uematsu *et al.* (2001) using a vortex method. Vibration and buckling analysis of composite cylindrical shells conveying hot fluid were studied by Kadoli and Ganesan (2003) using semi-analytical finite element method. Patel *et al.* (2006) investigated static and dynamic instability behaviors of stiffened shell panels under the uniform in-plane harmonic edge loading based on Hill's infinite determinant. Axial stability of cylindrical shell with an elastic core was investigated by Ghorbanpour Arani *et al.* (2007) using energy method. Nonlinear dynamics behaviours of pipes conveying pulsating fluid was investigated by Wang (2009) using Runge-Kutta scheme. Vibration analysis of CNTs

reinforced composites was presented by Formica *et al.* (2010) employing Eshelby-Mori-Tanaka approach. Donnell shell model in conjunction with the beam models, the transverse vibrations of single and double-walled CNTs are investigated by Ghorbanpour Arani *et al.* (2010). De Bellis *et al.* (2010) considered the behaviour of a fluid conveying pipe on a partial elastic foundation based on Timoshenko beam model. Using the Amabili-Reddy higher-order shear deformation theory, Amabili (2011) presented nonlinear forced vibration of laminated circular cylindrical shells by Lagrange method. Buckling analysis of laminated composite plates reinforced by SWCNTs was carried out by Ghorbanpour Arani *et al.* (2011a) using an analytical approach as well as the finite element method. Mohammadi and Sedaghati (2012) presented vibration response and its optimization of viscoelastic sandwich cylindrical shell. A closed-form formulation based on 3D refined higher-order shear deformation theory was presented by Khalili *et al.* (2012) for free vibration analysis of laminated composite shell was investigated by Kumar *et al.* (2013b) using an efficient 2D finite element (FE) model based on higher order zigzag theory. Analyzing the vibration of circular cylindrical shells subjected to different boundary conditions. Influence of latitude wind pressure distribution on the responses of hyperboloidal cooling tower shell was presented by Zhang *et al.* (2013). In numerical modeling procedure, soil parameters were modeled by Srivastava and Sivakumar Babu (2011) as two-dimensional non-Gaussian homogeneous random field using Cholesky decomposition technique. Static analysis of laminated composite and

\*Corresponding author, Ph.D. Student,  
E-mail: [h.rahimipour@nioc.ir](mailto:h.rahimipour@nioc.ir)

sandwich shell was presented by Kumar *et al.* (2013a) developing a C0 finite element (FE) formulation based on higher order zigzag theory (HOZT) using Sander's approximations. An another work by Kumar *et al.* (2013b), free vibration analysis of laminated composite skew hyper shells were presented using a C0 FE formulation based on HSDT where the isoparametric FE used in the present model consists of nine nodes with seven nodal unknowns per node. Using Navier-type closed-form solution, Mantari and Guedes Soares (2014) presented the optimization of the sinusoidal higher order shear deformation theory (HSDT) for the bending analysis of functionally graded shells. Forced vibration response of laminated composite and sandwich shell was studied by Kumar *et al.* (2014) using a 2D FE (finite element) model based on higher order zigzag theory (HOZT). Liew *et al.* (2014) studied postbuckling analysis of CNT-reinforced functionally graded cylindrical panels using a meshless approach. Lei *et al.* (2014) used the mesh-free kp-Ritz for dynamic stability analysis of CNT-reinforced functionally graded cylindrical panels under static and periodic axial force. Nonlinear behaviour of CNT-reinforced functionally graded cylindrical panels was addressed by Zhang *et al.* (2014a) based on the Eshelby-Mori-Tanaka approach. Zhang *et al.* (2014b) employed mesh-free kp-Ritz for vibration analysis of CNT reinforced composite cylindrical panels based on FSDT. Nonlinear vibration and dynamic response of imperfect eccentrically stiffened functionally graded thick circular cylindrical shells were studied by Duc and Than (2015) using both the FSDT and stress function. Based on FSDT, Yang *et al.* (2015) studied free vibration and damping analysis of thick sandwich cylindrical shells with a viscoelastic core. Vibration analysis of cylindrical shells conveying fluid was studied by Seo *et al.* (2015) using FE method. Static stresses analysis of CNT reinforced composite cylinder was investigated by Ghorbanpour Arani *et al.* (2015a). A C0 FE formulation based on HSDT was developed by Kumar *et al.* (2013c) for free vibration analysis of composite skew cylindrical shells. A new reinforcing element including the elements (anchors) attached to the ordinary geogrid for increasing the pull-out resistance of the reinforcement, was used by Mahdi and Katebi (2015). Vibration analysis of embedded functionally graded (FG)-carbon nanotubes (CNT)-reinforced piezoelectric cylindrical shell subjected to uniform and non-uniform temperature distributions were presented by Madani *et al.* (2016).

Considering the immense advantages offered by piezoelectric structures, Tzou and Gadre (1989) proposed a multi-layered thin shell integrated with PVDF actuator layers based on Hamilton's principle. Based on Hamilton's principle, Maxwell equation and FSDT, Sheng and Wang (2010) studied free vibration and buckling of the functionally graded piezoelectric cylindrical shell. Alibeigloo and Kani (2010) focused on the vibration analysis of hybrid laminated shell with various boundary conditions based on an analytical solution for simply supported boundary condition and DQM for the other boundary conditions. Ghorbanpour Arani *et al.* (2011b) studied electro-thermo-mechanical stress analysis of rotating functionally graded piezoelectric cylinders.

Ghorbanpour Arani *et al.* (2012) studied nonlinear vibration of embedded piezoelectric composite microtube conveying fluid based on Reddy beam theory. In another work by the same authors (2013), nonlinear vibration and instability of embedded double-walled boron nitride nanotubes based on nonlocal cylindrical shell theory were presented. Ghorbanpour Arani *et al.* (2013a) studied electro-thermo-elastic stress analysis of piezoelectric polymeric thick-walled cylinder reinforced by BNNT. Ghorbanpour Arani *et al.* (2015b) investigated electro-thermal nonlinear vibration and stability of a embedded smart composite micro-tube reinforced by Boron-Nitride nanotubes (BNNTs). Viscous fluid induced nonlinear free vibration and instability analysis of a functionally graded carbon nanotube-reinforced composite (CNTRC) cylindrical shell integrated with two uniformly distributed piezoelectric layers on the top and bottom surfaces of the cylindrical shell were presented by Rabani Bidgoli *et al.* (2016).

To the best of our knowledge, the mechanical analyses of separators however have not received enough attentions so far. Motivated by these considerations, in order to optimize the separators designing, our end is to investigate pulsating fluid induced dynamic stability of piezoelectric separators reinforced with SWCNTs. The elastic medium is simulated with nonlinear orthotropic visco-Pasternak medium. The Kelvin-Voigt model is assumed for incorporating the structural damping effects. CST, FSDT and SSDT are applied for obtaining the motion equations. The separator is subjected to 2D magnetic and 3D electric fields for smart dynamic stability control of structure. DQM in conjunction with Bolotin's method is used for calculating DIR. The effects of external voltage, magnetic field, visco-Pasternak foundation, structural damping and volume percent of SWCNTs on the dynamic stability of separator are shown.

## 2. Mathematical modeling

Consider a piezoelectric separator modeled with cylindrical shell as depicted in Fig. 1 in which geometrical parameters of length  $L$ , radius  $R$  and thickness  $h$  are indicated. The cylindrical coordinate is considered in the middle surface of shell in which  $x$ ,  $\theta$  and  $z$  represent the axial, circumferential and radial directions, respectively.

### 2.1 CST

Based on CST, the displacement components of an arbitrary point in three directions may be written as (Amabili 2008)

$$u_1(x, \theta, z, t) = u(x, \theta, t) - z \frac{\partial w(x, \theta, t)}{\partial x}, \quad (1a)$$

$$u_2(x, \theta, z, t) = v(x, \theta, t) - z \frac{\partial w(x, \theta, t)}{R \partial \theta}, \quad (1b)$$

$$u_3(x, \theta, z, t) = w(x, \theta, t), \quad (1c)$$

where  $u(x, \theta, t)$ ,  $v(x, \theta, t)$  and  $w(x, \theta, t)$  are translations of a

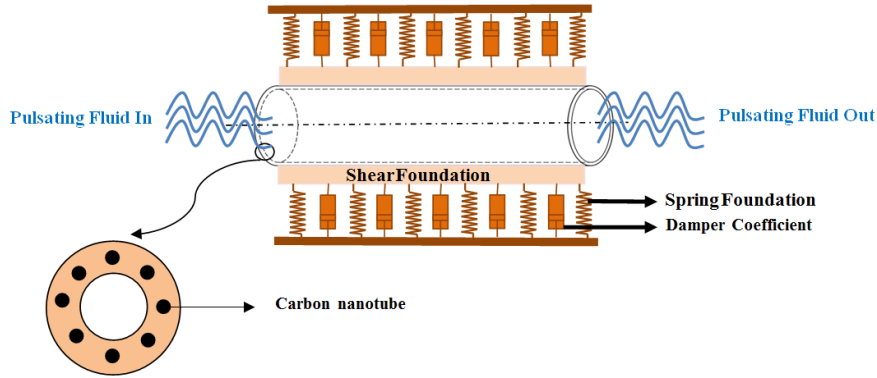


Fig. 1 A schematic figure for piezoelectric nano-composite separator conveying pulsating fluid

point at the middle-surface of the shell. Using Donnell’s theory, the nonlinear strain-displacement relations may be expressed as

$$\varepsilon_{xx} = \frac{\partial u}{\partial x} + \frac{1}{2} \left( \frac{\partial w}{\partial x} \right)^2 - z \frac{\partial^2 w}{\partial x^2}, \quad (2a)$$

$$\varepsilon_{\theta\theta} = \frac{\partial v}{R\partial\theta} + \frac{w}{R} + \frac{1}{2} \left( \frac{\partial w}{R\partial\theta} \right)^2 - z \frac{\partial^2 w}{R^2\partial\theta^2}, \quad (2b)$$

$$\gamma_{x\theta} = \frac{\partial u}{R\partial\theta} + \frac{\partial v}{\partial x} + \frac{\partial w}{\partial x} \frac{\partial w}{R\partial\theta} - 2z \frac{\partial^2 w}{R\partial x\partial\theta}. \quad (2c)$$

### 2.2 FSDT

Based on FSDT, the displacement field can be expressed as may be written as (Amabili 2008)

$$u_1(x, \theta, z, t) = u(x, \theta, t) + z\psi_x(x, \theta, t), \quad (3a)$$

$$u_2(x, \theta, z, t) = v(x, \theta, t) + z\psi_\theta(x, \theta, t), \quad (3b)$$

$$u_3(x, \theta, z, t) = w(x, \theta, t), \quad (3c)$$

where  $\psi_x(x, \theta, t)$  and  $\psi_\theta(x, \theta, t)$  are the rotations of the normal to the mid-plane about  $x$ - and  $\theta$ - directions, respectively. However, the nonlinear strain-displacement relations associated with the above displacement field can be derived as

$$\varepsilon_{xx} = \frac{\partial u}{\partial x} + \frac{1}{2} \left( \frac{\partial w}{\partial x} \right)^2 + z \frac{\partial \psi_x}{\partial x}, \quad (4a)$$

$$\varepsilon_{\theta\theta} = \frac{\partial v}{R\partial\theta} + \frac{w}{R} + \frac{1}{2} \left( \frac{\partial w}{R\partial\theta} \right)^2 + z \frac{\partial \psi_\theta}{R\partial\theta}, \quad (4b)$$

$$\gamma_{\alpha z} = \frac{\partial w}{R\partial\theta} - \frac{v}{R} + \psi_\theta, \quad (4c)$$

$$\gamma_{xz} = \frac{\partial w}{\partial x} + \psi_x, \quad (4d)$$

$$\gamma_{x\theta} = \frac{\partial v}{\partial x} + \frac{\partial u}{R\partial\theta} + \frac{\partial w}{\partial x} \frac{\partial w}{R\partial\theta} + z \left( \frac{\partial \psi_x}{R\partial\theta} + \frac{\partial \psi_\theta}{\partial x} \right). \quad (4e)$$

### 2.3 SSDT

Based on SSDT, the displacement field can be obtained using Eq. (5) as (Thai and Vo 2013)

$$u_1(x, \theta, z, t) = u(x, \theta, t) - z \frac{\partial w_b(x, \theta, t)}{\partial x} - f \frac{\partial w_s(x, \theta, t)}{\partial x}, \quad (5a)$$

$$u_2(x, \theta, z, t) = v(x, \theta, t) - z \frac{\partial w_b(x, \theta, t)}{R\partial\theta} - f \frac{\partial w_s(x, \theta, t)}{R\partial\theta}, \quad (5b)$$

$$u_3(x, \theta, z, t) = w_b(x, \theta, t) + w_s(x, \theta, t), \quad (5c)$$

where  $f = z - \frac{h}{\pi} \sin \frac{\pi z}{h}$ ;  $w_b(x, \theta, t)$  and  $w_s(x, \theta, t)$  are the bending and shear components of transverse displacement. The nonlinear kinematic relations can be expressed as follows

$$\varepsilon_{xx} = \frac{\partial u}{\partial x} + \frac{1}{2} \left( \frac{\partial w_b}{\partial x} \right)^2 + \frac{1}{2} \left( \frac{\partial w_s}{\partial x} \right)^2 - z \frac{\partial^2 w_b}{\partial x^2} - f \frac{\partial^2 w_s}{\partial x^2}, \quad (6a)$$

$$\varepsilon_{\theta\theta} = \frac{\partial v}{R\partial\theta} + \frac{w_b}{R} + \frac{w_s}{R} + \frac{1}{2} \left( \frac{\partial w_b}{R\partial\theta} \right)^2 + \frac{1}{2} \left( \frac{\partial w_s}{R\partial\theta} \right)^2 + \frac{1}{2} \left( \frac{\partial w_s}{R\partial\theta} \right)^2 - z \frac{\partial^2 w_b}{R^2\partial\theta^2} - f \frac{\partial^2 w_b}{R^2\partial\theta^2}, \quad (6b)$$

$$\gamma_{\alpha z} = p \frac{\partial w_s}{R\partial\theta} - \frac{v}{R}, \quad (6c)$$

$$\gamma_{xz} = p \frac{\partial w_s}{\partial x}, \quad (6d)$$

$$\gamma_{x\theta} = \frac{\partial u}{R\partial\theta} + \frac{\partial v}{\partial x} + \left( \frac{\partial w_b}{\partial x} + \frac{\partial w_s}{\partial x} \right) \left( \frac{\partial w_b}{R\partial\theta} + \frac{\partial w_s}{R\partial\theta} \right) - 2z \frac{\partial^2 w_b}{R\partial x\partial\theta} - 2f \frac{\partial^2 w_s}{R\partial x\partial\theta}, \quad (6e)$$

where  $p = \cos \frac{\pi z}{h}$ .

### 3. Constitutive equations for piezoelectric separator

As it is well known, applying an electric field and mechanical displacement to piezoelectric materials yield a mechanical displacement and voltage, respectively. However, the constitutive equation includes stresses  $\sigma$  and strains  $\varepsilon$  tensors on the mechanical side, as well as flux density  $D$  and field strength  $E$  tensors on the electrostatic side, which may be combined with each other as follows (Ghorbanpour Arani *et al.* 2013b)

$$\sigma_{ij} = C_{ijkl} \varepsilon_{kl} - e_{ijm} E_m, \quad (7)$$

$$D_i = e_{ijm} \varepsilon_{jm} + \varepsilon_{im} E_m, \quad (8)$$

where  $C_{ijkl}$ ,  $e_{ijm}$ ,  $\varepsilon_{im}$  are elastic constants, piezoelectric constants, dielectric constants, respectively, which can be determined for separator reinforced with SWCNT from Mixture's rule. In addition,  $E_m$  ( $m = x, \theta, z$ ) representing electric field which can be defined as a function of electric potential as (Ghorbanpour Arani *et al.* 2015c)

$$E_x = -\frac{\partial \phi}{\partial x}, E_\theta = -\frac{\partial \phi}{R \partial \theta}, E_z = -\frac{\partial \phi}{\partial z}. \quad (9)$$

The above equations for CST may be simplified as

$$\begin{bmatrix} \sigma_{xx} \\ \sigma_{\theta\theta} \\ \tau_{x\theta} \end{bmatrix} = \begin{bmatrix} C_{11} & C_{12} & 0 \\ C_{12} & C_{22} & 0 \\ 0 & 0 & C_{66} \end{bmatrix} \begin{bmatrix} \varepsilon_{xx} \\ \varepsilon_{\theta\theta} \\ \gamma_{x\theta} \end{bmatrix} - \begin{bmatrix} 0 & 0 & e_{31} \\ 0 & 0 & e_{32} \\ 0 & 0 & 0 \end{bmatrix} \begin{bmatrix} E_x \\ E_\theta \\ E_z \end{bmatrix}, \quad (10)$$

$$\begin{bmatrix} D_x \\ D_\theta \\ D_z \end{bmatrix} = \begin{bmatrix} 0 & 0 & 0 \\ 0 & 0 & 0 \\ e_{31} & e_{32} & 0 \end{bmatrix} \begin{bmatrix} \varepsilon_{xx} \\ \varepsilon_{\theta\theta} \\ \gamma_{x\theta} \end{bmatrix} + \begin{bmatrix} \varepsilon_{11} & 0 & 0 \\ 0 & \varepsilon_{22} & 0 \\ 0 & 0 & \varepsilon_{33} \end{bmatrix} \begin{bmatrix} E_x \\ E_\theta \\ E_z \end{bmatrix}. \quad (11)$$

Eqs. (7) and (8) for FSDT and SSDT can be simplified as

$$\begin{bmatrix} \sigma_{xx} \\ \sigma_{\theta\theta} \\ \tau_{\theta z} \\ \tau_{xz} \\ \tau_{x\theta} \end{bmatrix} = \begin{bmatrix} C_{11} & C_{12} & 0 & 0 & 0 \\ C_{12} & C_{22} & 0 & 0 & 0 \\ 0 & 0 & C_{44} & 0 & 0 \\ 0 & 0 & 0 & C_{55} & 0 \\ 0 & 0 & 0 & 0 & C_{66} \end{bmatrix} \begin{bmatrix} \varepsilon_{xx} \\ \varepsilon_{\theta\theta} \\ \gamma_{\theta z} \\ \gamma_{xz} \\ \gamma_{x\theta} \end{bmatrix} - \begin{bmatrix} 0 & 0 & e_{31} \\ 0 & 0 & e_{32} \\ 0 & e_{24} & 0 \\ e_{15} & 0 & 0 \\ 0 & 0 & 0 \end{bmatrix} \begin{bmatrix} E_x \\ E_\theta \\ E_z \end{bmatrix}, \quad (12)$$

$$\begin{bmatrix} D_x \\ D_\theta \\ D_z \end{bmatrix} = \begin{bmatrix} 0 & 0 & 0 & e_{15} & 0 \\ 0 & 0 & e_{24} & 0 & 0 \\ e_{31} & e_{32} & 0 & 0 & 0 \end{bmatrix} \begin{bmatrix} \varepsilon_{xx} \\ \varepsilon_{\theta\theta} \\ \gamma_{\theta z} \\ \gamma_{xz} \\ \gamma_{x\theta} \end{bmatrix} + \begin{bmatrix} \varepsilon_{11} & 0 & 0 \\ 0 & \varepsilon_{22} & 0 \\ 0 & 0 & \varepsilon_{33} \end{bmatrix} \begin{bmatrix} E_x \\ E_\theta \\ E_z \end{bmatrix}. \quad (13)$$

The electric potential distribution in the thickness direction of the piezoelectric separator can be assumed as follows which satisfying the Maxwell equation (Ghorbanpour Arani *et al.* 2015b)

$$\Phi(x, \theta, z, t) = -\cos\left(\frac{\pi z}{h}\right) \phi(x, \theta, t) + \frac{2V_0 z}{h}, \quad (14)$$

where  $V_0$  is external electric voltage. Substituting Eq. (14) into Eq. (9) yields

$$E_x = \cos\left(\frac{\pi z}{h}\right) \frac{\partial \phi}{\partial x}, \quad (15a)$$

$$E_\theta = \cos\left(\frac{\pi z}{h}\right) \frac{\partial \phi}{R \partial \theta}, \quad (15b)$$

$$E_z = -\frac{\pi}{h} \sin\left(\frac{\pi z}{h}\right) \phi - \frac{2V_0}{h}. \quad (15c)$$

Based on Kelvin-Voigt (Ghorbanpour Arani *et al.* 2015b) model, the elastic constant of structure can be defined as

$$C_{ij}^{(k)} = C_{ij}^{(k)} \left(1 + g \frac{\partial}{\partial t}\right), \quad (16)$$

where  $g$  is structural damping parameter. In the above equations, the effect of viscoelasticity in mechanical form has been considered and electrical Hysteresis effect (Jalili 2010) has been ignored.

### 4. Mixture method

According to mixture rule, the effective Young and shear moduli of nano-composite structure can be expressed as (Zhang *et al.* 2014a)

$$E_{11} = \eta_1 V_{CNT} E_{r11} + (1 - V_{CNT}) E_m, \quad (17a)$$

$$\frac{\eta_2}{E_{22}} = \frac{V_{CNT}}{E_{r22}} + \frac{(1 - V_{CNT})}{E_m}, \quad (17b)$$

$$\frac{\eta_3}{G_{12}} = \frac{V_{CNT}}{G_{r12}} + \frac{(1 - V_{CNT})}{G_m}, \quad (17c)$$

where  $E_{r11}$ ,  $E_{r22}$  and  $G_{r11}$  indicate the Young's moduli and shear modulus of SWCNTs, respectively,  $E$ , and  $G_m$  represent the Young's moduli and shear modulus the matrix;  $\eta_j$  ( $j = 1, 2, 3$ ) is the SWCNTs efficiency parameter;  $V_{CNT}$  and  $V_m$  are the volume fractions of the CNTs and matrix, respectively, which are

$$V_{CNT} = \frac{w_{CNT}}{w_{CNT} + (\rho_{CNT} / \rho_m) - (\rho_{CNT} / \rho_m) w_{CNT}}, \quad (18)$$

$$V_m = 1 - V_{CNT},$$

where  $w_{CNT}$ ,  $\rho_m$  and  $\rho_{CNT}$  are the mass fraction of the SWCNTs, the densities of the matrix and SWCNTs, respectively. Similarly, the density ( $\rho$ ) of the structure can be obtained as follows

$$\rho = V_{CNT}\rho_f + V_m\rho_m, \quad (19)$$

where  $\nu_{r12}$  and  $\nu_m$  are Poisson's ratios of the SWCNT and matrix, respectively.

## 5. Energy method

In this section, energy method and Hamilton's principal are used for obtaining the motion equations. The total potential energy of the structure is the sum of potential energy,  $U$ , kinetic energy,  $K$  and the work done by the external forces,  $W$  which may be written generally as

$$U = \frac{1}{2} \int \sigma_{ij} \varepsilon_{ij} dV, \quad (20)$$

$$K = \frac{\rho}{2} \int ((\dot{u}_1)^2 + (\dot{u}_2)^2 + (\dot{u}_3)^2) dV, \quad (21)$$

$$W = \int qwdA. \quad (22)$$

### 5.1 CST

The potential energy of CST can be obtained by substituting Eqs. (10) and (11) into Eq. (20) as follows

$$\begin{aligned} U = & 0.5 \int \left[ N_{xx} \left( \frac{\partial u}{\partial x} + \frac{1}{2} \left( \frac{\partial w}{\partial x} \right)^2 \right) \right. \\ & + N_{\theta\theta} \left( \frac{\partial v}{R\partial\theta} + \frac{w}{R} + \frac{1}{2} \left( \frac{\partial w}{R\partial\theta} \right)^2 \right) + N_{x\theta} \left( \frac{\partial u}{R\partial\theta} + \frac{\partial v}{\partial x} + \frac{\partial w}{R\partial\theta} \frac{\partial w}{\partial x} \right) \\ & - M_{xx} \frac{\partial^2 w}{\partial x^2} - M_{\theta\theta} \frac{\partial^2 w}{R^2 \partial \theta^2} - 2M_{x\theta} \frac{\partial^2 w}{R\partial\theta\partial x} \Big] dA \\ & - 0.5 \int \left[ D_x \left( \cos\left(\frac{\pi z}{h}\right) \frac{\partial \phi}{\partial x} \right) + D_\theta \left( \cos\left(\frac{\pi z}{h}\right) \frac{\partial \phi}{R\partial\theta} \right) \right. \\ & \left. + D_z \left( -\frac{\pi}{h} \sin\left(\frac{\pi z}{h}\right) \phi - \frac{2V_0}{h} \right) \right] dz dA. \end{aligned} \quad (23)$$

The kinetic energy of CST can be obtained by substituting Eq. (1) into Eq. (21) as follows

$$\begin{aligned} K = & 0.5 \int \left[ I_0 \left( \left( \frac{\partial u}{\partial t} \right)^2 + \left( \frac{\partial v}{\partial t} \right)^2 + \left( \frac{\partial w}{\partial t} \right)^2 \right) \right. \\ & - 2I_1 \left( \frac{\partial u}{\partial t} \frac{\partial^2 w}{\partial t \partial x} + \frac{\partial v}{\partial t} \frac{\partial^2 w}{R\partial\theta} \right) \\ & \left. + I_2 \left( \left( \frac{\partial^2 w}{\partial t \partial x} \right)^2 + \left( \frac{\partial^2 w}{R^2 \partial t^2 \partial \theta^2} \right)^2 \right) \right] dA. \end{aligned} \quad (24)$$

The external works can be induced by nonlinear orthotropic visco-Pasternak medium, pulsating fluid in the separator and 2D magnetic fields due to the existence of SWCNTs. The force induced by nonlinear orthotropic visco-Pasternak foundation can be written as (Ghorbanpour

Arani *et al.* 2015b)

$$\begin{aligned} q_e = & -k_{1w}w - k_{2w}w^3 - c_d\dot{w} \\ & + k_{g\xi} \left( \cos^2\theta \frac{\partial^2 w}{\partial x^2} + 2\cos\theta \sin\theta \frac{\partial^2 w}{\partial x \partial y} + \sin^2\theta \frac{\partial^2 w}{\partial y^2} \right) \\ & + k_{g\zeta} \left( \sin^2\theta \frac{\partial^2 w}{\partial x^2} - 2\sin\theta \cos\theta \frac{\partial^2 w}{\partial x \partial y} + \cos^2\theta \frac{\partial^2 w}{\partial y^2} \right), \end{aligned} \quad (25)$$

where angle  $\theta$  describes the local  $\xi$  direction of orthotropic foundation with respect to the global  $x$ -axis of the system;  $k_{1w}$ ,  $k_{2w}$ ,  $c_d$ ,  $k_{g\xi}$  and  $k_{g\zeta}$ , respectively are linear spring, nonlinear spring, damper,  $\xi$ -shear and  $\zeta$ -shear constants.

The force induced by internal fluid may be described by the well-known Navier-Stokes equation as follows

$$\rho_f \frac{dV}{dt} = -\nabla P + \mu \nabla^2 V + F_{body}, \quad (26)$$

where  $V \equiv (v_z, v_\theta, v_x)$  is the flow velocity vector in polar coordinate;  $\frac{D}{Dt}$  is the material or total derivative;  $P$ ,  $\mu$  and  $\rho_f$  are the pressure, viscosity and mass density of the fluid, respectively;  $F_{body}$  represents the body forces. After some mathematical operations, the external work of the fluid can be expressed as

$$\begin{aligned} q_f = & -\rho_f \left( \frac{\partial^2 w}{\partial t^2} + 2v_x \frac{\partial^2 w}{\partial x \partial t} + v_x^2 \frac{\partial^2 w}{\partial x^2} \right) \\ & + \mu \left( \frac{\partial^3 w}{\partial x^2 \partial t} + \frac{\partial^3 w}{R^2 \partial \theta^2 \partial t} + v_x \left( \frac{\partial^3 w}{\partial x^3} + \frac{\partial^3 w}{R^2 \partial \theta^2 \partial x} \right) \right). \end{aligned} \quad (27)$$

The pulsating internal flow is assumed harmonically as follows

$$V_x = V_0(1 + \beta \cos(\omega t)), \quad (28)$$

where  $V_0$ ,  $\beta$  and  $\omega$  are the mean flow velocity, the harmonic amplitude and pulsation frequency, respectively. The Lorentz force due to a steady magnetic field,  $H_0$  can be obtained as follows (Ghorbanpour Arani *et al.* 2015b)

$$f_m = \eta \underbrace{\left( \nabla \times (\nabla \times (u \times H_0)) \right)}_J \times H_0, \quad (29)$$

where  $\eta$ ,  $\nabla$ ,  $u$ ,  $h$  and  $J$  are the magnetic permeability of the SWCNTs, gradient operator, displacement field vector, disturbing vectors of magnetic field and current density, respectively. Noted that in this paper the magnetic field is assumed as  $H_0 = H_x \delta_{xg} \bar{e}_x + H_\theta \delta_{\theta g} \bar{e}_\theta$  where  $\delta$  is the Kronecker delta tensor. Using Eqs. (1a)-(1c), the Lorentz force per unit volume can be calculated as

$$f_x = \eta H_\theta^2 \delta_{\theta g} \left[ \left( \frac{\partial^2 u}{\partial x^2} + \frac{\partial^2 u}{R^2 \partial \theta^2} \right) - z \left( \frac{\partial^3 w}{\partial x^3} + \frac{\partial^3 w}{R^2 \partial x \partial \theta^2} \right) \right], \quad (30a)$$

$$f_\theta = \eta H_x^2 \delta_{xg} \left[ \left( \frac{\partial^2 v}{\partial x^2} + \frac{\partial^2 v}{R^2 \partial \theta^2} \right) - z \left( \frac{\partial^3 w}{R^3 \partial \theta^3} + \frac{\partial^3 w}{R \partial \theta \partial x^2} \right) \right], \quad (30b)$$

$$f_z = \eta \left[ H_\theta^2 \delta_{\theta\theta} \left( \frac{\partial^2 w}{R^2 \partial \theta^2} - \frac{\partial^2 w}{\partial x^2} \right) + H_x^2 \delta_{x\theta} \left( \frac{\partial^2 w}{\partial x^2} - \frac{\partial^2 w}{R^2 \partial \theta^2} \right) \right] \quad (30c)$$

The generated forces and the bending moment caused by Lorentz force may be calculated by

$$(R_x^m, R_\theta^m, R_z^m) = \int_{-h/2}^{h/2} (f_x, f_\theta, f_z) dz, \quad (31)$$

$$(M_x^m, M_\theta^m, M_z^m) = \int_{-h/2}^{h/2} (f_x, f_\theta, f_z) z dz, \quad (32)$$

as a results

$$R_x^m = \eta h H_\theta^2 \delta_{\theta\theta} \left( \frac{\partial^2 u}{\partial x^2} + \frac{\partial^2 u}{R^2 \partial \theta^2} \right), \quad (33a)$$

$$R_\theta^m = \eta h H_x^2 \delta_{x\theta} \left( \frac{\partial^2 v}{\partial x^2} + \frac{\partial^2 v}{R^2 \partial \theta^2} \right), \quad (33b)$$

$$R_z^m = \eta h \left[ H_\theta^2 \delta_{\theta\theta} \left( \frac{\partial^2 w}{R^2 \partial \theta^2} - \frac{\partial^2 w}{\partial x^2} \right) + H_x^2 \delta_{x\theta} \left( \frac{\partial^2 w}{\partial x^2} - \frac{\partial^2 w}{R^2 \partial \theta^2} \right) \right], \quad (33c)$$

$$M_x^m = -\frac{\eta h^3 H_\theta^2}{12} \delta_{\theta\theta} \left( \frac{\partial^3 w}{\partial x^3} + \frac{\partial^3 w}{R^2 \partial x \partial \theta^2} \right), \quad (34a)$$

$$M_\theta^m = -\frac{\eta h^3 H_x^2}{12} \delta_{x\theta} \left( \frac{\partial^3 w}{R^3 \partial \theta^3} + \frac{\partial^3 w}{R \partial \theta \partial x^2} \right). \quad (34b)$$

## 5.2 FSDT

Combining of Eqs. (12), (13) and (20) yields the potential energy of FSDT as follows

$$\begin{aligned} U = 0.5 \int & \left[ N_{xx} \left( \frac{\partial u}{\partial x} + \frac{1}{2} \left( \frac{\partial w}{\partial x} \right)^2 \right) \right. \\ & + N_{\theta\theta} \left( \frac{\partial v}{R \partial \theta} + \frac{w}{R} + \frac{1}{2} \left( \frac{\partial w}{R \partial \theta} \right)^2 \right) \\ & + Q_\theta \left( \frac{\partial w}{R \partial \theta} - \frac{v}{R} + \psi_\theta \right) \left. \right] + Q_x \left( \frac{\partial w}{\partial x} + \psi_x \right) \\ & + N_{x\theta} \left( \frac{\partial v}{\partial x} + \frac{\partial u}{R \partial \theta} + \frac{\partial w}{\partial x} \frac{\partial w}{R \partial \theta} \right) + M_{xx} \frac{\partial \psi_x}{\partial x} \quad (35) \\ & + M_{\theta\theta} \frac{\partial \psi_\theta}{R \partial \theta} + M_{x\theta} \left( \frac{\partial \psi_x}{R \partial \theta} + \frac{\partial \psi_\theta}{\partial x} \right) \Big] dA \\ & - 0.5 \int \left[ D_x \left( \cos \left( \frac{\pi z}{h} \right) \frac{\partial \phi}{\partial x} \right) + D_\theta \left( \cos \left( \frac{\pi z}{h} \right) \frac{\partial \phi}{R \partial \theta} \right) \right. \\ & \left. + D_z \left( -\frac{\pi}{h} \sin \left( \frac{\pi z}{h} \right) \phi - \frac{2V_0}{h} \right) \right] dz dA. \end{aligned}$$

The kinetic energy of FSDT can be obtained by substituting Eq. (3) into Eq. (21) as follows

$$\begin{aligned} K = 0.5 \int & \left[ I_0 \left( \left( \frac{\partial u}{\partial t} \right)^2 + \left( \frac{\partial v}{\partial t} \right)^2 + \left( \frac{\partial w}{\partial t} \right)^2 \right) \right. \\ & + 2I_1 \left( \frac{\partial u}{\partial t} \frac{\partial \psi_x}{\partial t} + \frac{\partial v}{\partial t} \frac{\partial \psi_\theta}{\partial t} \right) \\ & \left. + I_2 \left( \left( \frac{\partial \psi_x}{\partial t} \right)^2 + \left( \frac{\partial \psi_\theta}{\partial t} \right)^2 \right) \right] dA. \quad (36) \end{aligned}$$

Using Eq. (3), the Lorentz force per unit volume for FSDT can be expressed as

$$f_x = \eta H_\theta^2 \delta_{\theta\theta} \left[ \left( \frac{\partial^2 u}{\partial x^2} + \frac{\partial^2 u}{R^2 \partial \theta^2} \right) + z \left( \frac{\partial^2 \psi_x}{\partial x^2} + \frac{\partial^2 \psi_x}{R^2 \partial \theta^2} \right) \right], \quad (37a)$$

$$f_\theta = \eta H_x^2 \delta_{x\theta} \left[ \left( \frac{\partial^2 v}{\partial x^2} + \frac{\partial^2 v}{R^2 \partial \theta^2} \right) + z \left( \frac{\partial^2 \psi_\theta}{R^2 \partial \theta^2} + \frac{\partial^2 \psi_\theta}{\partial x^2} \right) \right], \quad (37b)$$

$$f_z = \eta \left[ H_\theta^2 \delta_{\theta\theta} \left( \frac{\partial^2 w}{\partial x^2} + \frac{\partial \psi_\theta}{R \partial \theta} \right) + H_x^2 \delta_{x\theta} \left( \frac{\partial^2 w}{\partial x^2} + \frac{\partial \psi_\theta}{R \partial \theta} \right) \right]. \quad (37c)$$

However, using Eqs. (31) and (32), the generated forces and the bending moment caused by Lorentz force may be calculated by

$$R_x^m = \eta h H_\theta^2 \delta_{\theta\theta} \left( \frac{\partial^2 u}{\partial x^2} + \frac{\partial^2 u}{R^2 \partial \theta^2} \right), \quad (38a)$$

$$R_\theta^m = \eta h H_x^2 \delta_{x\theta} \left( \frac{\partial^2 v}{\partial x^2} + \frac{\partial^2 v}{R^2 \partial \theta^2} \right), \quad (38b)$$

$$R_z^m = \eta h \left[ H_\theta^2 \delta_{\theta\theta} \left( \frac{\partial^2 w}{\partial x^2} + \frac{\partial \psi_\theta}{R \partial \theta} \right) + H_x^2 \delta_{x\theta} \left( \frac{\partial^2 w}{\partial x^2} + \frac{\partial \psi_\theta}{R \partial \theta} \right) \right], \quad (38c)$$

$$M_x^m = \frac{\eta h^3 H_\theta^2}{12} \delta_{\theta\theta} \left( \frac{\partial^2 \psi_x}{\partial x^2} + \frac{\partial^2 \psi_x}{R^2 \partial \theta^2} \right), \quad (39a)$$

$$M_\theta^m = \frac{\eta h^3 H_x^2}{12} \delta_{x\theta} \left( \frac{\partial^2 \psi_\theta}{R^2 \partial \theta^2} + \frac{\partial^2 \psi_\theta}{\partial x^2} \right). \quad (39b)$$

Noted that the induced forces due to the viscoelastic foundation and pulsating fluid are the same as Eqs. (25) and (27), respectively.

## 5.3 SSST

Substituting Eqs. (12) and (13) into Eq. (20) yields the potential energy of SSST as follows

$$U = 0.5 \int \left[ N_{xx} \left( \frac{\partial u}{\partial x} + \frac{1}{2} \left( \frac{\partial w_b}{\partial x} \right)^2 + \frac{1}{2} \left( \frac{\partial w_s}{\partial x} \right)^2 \right) \right] \quad (40)$$

$$\begin{aligned}
 &+ N_{\theta\theta} \left( \frac{\partial v}{R\partial\theta} + \frac{w_b}{R} + \frac{w_s}{R} + \frac{1}{2} \left( \frac{\partial w_b}{R\partial\theta} \right)^2 + \frac{1}{2} \left( \frac{\partial w_s}{R\partial\theta} \right)^2 \right) \\
 &+ N_{x\theta} \left( \frac{\partial v}{\partial x} + \frac{\partial u}{R\partial\theta} + \left( \frac{\partial w_b}{\partial x} + \frac{\partial w_s}{\partial x} \right) \left( \frac{\partial w_b}{R\partial\theta} + \frac{\partial w_s}{R\partial\theta} \right) \right) \\
 &+ Q_\theta \frac{v}{R} - M_{xx} \left( \frac{\partial^2 w_b}{\partial x^2} \right) - M_{\theta\theta} \left( \frac{\partial^2 w_b}{R^2 \partial \theta^2} \right) \\
 &- 2M_{x\theta} Q_x \left( \frac{\partial^2 w_b}{R\partial\theta\partial x} \right) - S_{xx} \frac{\partial^2 w_s}{R x^2} - S_{\theta\theta} \frac{\partial^2 w_s}{R^2 \partial \theta^2} \\
 &- 2S_{x\theta} \frac{\partial^2 w_s}{R\partial\theta\partial x} + F_{\theta\theta} \frac{\partial w_s}{R\partial\theta} + F_{xx} \frac{\partial w_s}{R x} \Big) dA \\
 &- 0.5 \int \left( D_x \left( \cos \left( \frac{\pi z}{h} \right) \frac{\partial \varphi}{\partial x} \right) + D_\theta \left( \cos \left( \frac{\pi z}{h} \right) \frac{\partial \varphi}{R\partial\theta} \right) \right. \\
 &\left. + D_z \left( -\frac{\pi}{h} \sin \left( \frac{\pi z}{h} \right) \varphi - \frac{2V_0}{h} \right) \right) dz dA.
 \end{aligned} \tag{40}$$

The kinetic energy of SSDT can be obtained by substituting Eqs. (5) into Eq. (21) as follows

$$\begin{aligned}
 K = 0.5 \int & \left( I_0 \left( \left( \frac{\partial u}{\partial t} \right)^2 + \left( \frac{\partial v}{\partial t} \right)^2 + \left( \frac{\partial w_b}{\partial t} \right)^2 + \left( \frac{\partial w_s}{\partial t} \right)^2 \right. \right. \\
 &+ 2 \frac{\partial w_b}{\partial t} \frac{\partial w_s}{\partial t} \Big) - 2I_1 \left( \frac{\partial u}{\partial t} \frac{\partial^2 w_b}{\partial t \partial x} + \frac{\partial v}{\partial t} \frac{\partial^2 w_b}{R \partial t \partial \theta} \right) \\
 &+ I_2 \left( \left( \frac{\partial^2 w_b}{\partial t \partial x} \right)^2 + \left( \frac{\partial^2 w_b}{R \partial t \partial \theta} \right)^2 \right) \\
 &+ I_3 \left( \left( \frac{\partial^2 w_s}{\partial t \partial x} \right)^2 + \left( \frac{\partial^2 w_s}{R \partial t \partial \theta} \right)^2 \right) \\
 &+ 2I_4 \left( \frac{\partial^2 w_b}{\partial t \partial x} \frac{\partial^2 w_s}{\partial t \partial x} + \frac{\partial^2 w_b}{R \partial t \partial \theta} \frac{\partial^2 w_s}{R \partial t \partial \theta} \right) \\
 &+ 2I_5 \left( \frac{\partial u}{\partial t} \frac{\partial^2 w_s}{\partial t \partial x} + \frac{\partial v}{\partial t} \frac{\partial^2 w_s}{R \partial t \partial \theta} \right) \Big) dA.
 \end{aligned} \tag{41}$$

Using Eq. (5), the Lorentz force per unit volume for FSDT can be expressed as

$$\begin{aligned}
 f_x = \eta H_\theta^2 \delta_{\theta\theta} & \left[ \left( \frac{\partial^2 u}{\partial x^2} + \frac{\partial^2 u}{R^2 \partial \theta^2} \right) \right. \\
 & \left. - z \left( \frac{\partial^3 w_b}{\partial x^3} + \frac{\partial^3 w}{R^2 \partial x \partial \theta^2} \right) - f \left( \frac{\partial^3 w_s}{\partial x^3} + \frac{\partial^3 w_s}{R^2 \partial x \partial \theta^2} \right) \right],
 \end{aligned} \tag{42a}$$

$$\begin{aligned}
 f_\theta = \eta H_x^2 \delta_{x\theta} & \left[ \left( \frac{\partial^2 v}{\partial x^2} + \frac{\partial^2 v}{R^2 \partial \theta^2} \right) \right. \\
 & \left. - z \left( \frac{\partial^3 w_b}{R^3 \partial \theta^3} + \frac{\partial^3 w_b}{R \partial \theta \partial x^2} \right) - f \left( \frac{\partial^3 w_s}{R^3 \partial \theta^3} + \frac{\partial^3 w_s}{R \partial \theta \partial x^2} \right) \right],
 \end{aligned} \tag{42b}$$

$$\begin{aligned}
 f_z = \eta & \left[ H_\theta^2 \delta_{\theta\theta} \left( \frac{\partial^2 w_b}{R^2 \partial \theta^2} + \frac{\partial^2 w_s}{R^2 \partial \theta^2} - \frac{\partial^2 w_b}{\partial x^2} \right) \right. \\
 & \left. - (1-p) \frac{\partial^2 w_s}{\partial x^2} \right. \\
 & \left. + H_x^2 \delta_{x\theta} \left( \frac{\partial^2 w_b}{\partial x^2} + \frac{\partial^2 w_s}{\partial x^2} - \frac{\partial^2 w_b}{R^2 \partial \theta^2} \right) \right. \\
 & \left. - (1-p) \frac{\partial^2 w_s}{R^2 \partial \theta^2} \right].
 \end{aligned} \tag{42c}$$

However, using Eqs. (31) and (32), the generated forces and the bending moment caused by Lorentz force may be calculated by

$$R_x^m = \eta h H_\theta^2 \delta_{\theta\theta} \left( \frac{\partial^2 u}{\partial x^2} + \frac{\partial^2 u}{R^2 \partial \theta^2} \right), \tag{43a}$$

$$R_\theta^m = \eta h H_x^2 \delta_{x\theta} \left( \frac{\partial^2 v}{\partial x^2} + \frac{\partial^2 v}{R^2 \partial \theta^2} \right), \tag{43b}$$

$$\begin{aligned}
 R_z^m = \eta h & \left[ H_\theta^2 \delta_{\theta\theta} \left( \frac{\partial^2 w_b}{R^2 \partial \theta^2} + \frac{\partial^2 w_s}{R^2 \partial \theta^2} - \frac{\partial^2 w_b}{\partial x^2} \right) \right. \\
 & \left. - (1-\frac{2}{\pi}) \frac{\partial^2 w_s}{\partial x^2} \right. \\
 & \left. + H_x^2 \delta_{x\theta} \left( \frac{\partial^2 w_b}{\partial x^2} + \frac{\partial^2 w_s}{\partial x^2} - \frac{\partial^2 w_b}{R^2 \partial \theta^2} \right) \right. \\
 & \left. - (1-\frac{2}{\pi}) \frac{\partial^2 w_s}{R^2 \partial \theta^2} \right],
 \end{aligned} \tag{43c}$$

$$\begin{aligned}
 M_x^m = -\frac{\eta h^3 H_\theta^2}{12} \delta_{\theta\theta} & \left( \frac{\partial^3 w_b}{\partial x^3} + \frac{\partial^3 w_b}{R^2 \partial x \partial \theta^2} \right. \\
 & \left. + \frac{\partial^3 w_s}{\partial x^3} + \frac{\partial^3 w_s}{R^2 \partial x \partial \theta^2} \right) \\
 & + \frac{2\eta h^3 H_\theta^2}{\pi^3} \delta_{\theta\theta} \left( \frac{\partial^3 w_s}{\partial x^3} + \frac{\partial^3 w_s}{R^2 \partial x \partial \theta^2} \right),
 \end{aligned} \tag{44a}$$

$$\begin{aligned}
 M_\theta^m = -\frac{\eta h^3 H_x^2}{12} \delta_{x\theta} & \left( \frac{\partial^3 w_b}{R^3 \partial \theta^3} + \frac{\partial^3 w_b}{R \partial \theta \partial x^2} \right. \\
 & \left. + \frac{\partial^3 w_s}{R^3 \partial \theta^3} + \frac{\partial^3 w_s}{R \partial \theta \partial x^2} \right) \\
 & + \frac{2\eta h^3 H_\theta^2}{\pi^3} \delta_{x\theta} \left( \frac{\partial^3 w_s}{R^3 \partial \theta^3} + \frac{\partial^3 w_s}{R \partial \theta \partial x^2} \right).
 \end{aligned} \tag{44b}$$

Noted that the induced forces due to the viscoelastic foundation and pulsating fluid are the same as Eqs. (25) and (27), respectively.

In above relations, the resultant force and moments may be calculated as

$$\begin{bmatrix} N_{xx} \\ N_{\theta\theta} \\ N_{x\theta} \\ Q_x \\ Q_\theta \end{bmatrix} = \int_{-h/2}^{h/2} \begin{bmatrix} \sigma_{xx} \\ \sigma_{\theta\theta} \\ \sigma_{x\theta} \\ k' \sigma_{xz} \\ k' \sigma_{z\theta} \end{bmatrix} dz, \quad (45)$$

$$\begin{bmatrix} M_{xx} \\ M_{\theta\theta} \\ M_{x\theta} \end{bmatrix} = \int_{-h/2}^{h/2} \begin{bmatrix} \sigma_{xx} \\ \sigma_{\theta\theta} \\ \sigma_{x\theta} \end{bmatrix} z dz, \quad (46)$$

$$\begin{bmatrix} S_{xx} \\ S_{\theta\theta} \\ S_{x\theta} \end{bmatrix} = \int_{-h/2}^{h/2} \begin{bmatrix} \sigma_{xx} \\ \sigma_{\theta\theta} \\ \sigma_{x\theta} \end{bmatrix} f dz, \quad (47)$$

$$\begin{bmatrix} F_{xx} \\ F_{\theta\theta} \end{bmatrix} = \int_{-h/2}^{h/2} \begin{bmatrix} \sigma_{xx} \\ \sigma_{\theta\theta} \end{bmatrix} p dz, \quad (48)$$

where  $k'$  is shear correction factor which used in FSDT. Furthermore, the moment of inertia in kinetic energy of three theories can be defined as

$$(I_0, I_1, I_2, I_3, I_4, I_5) = \int_{-h/2}^{h/2} \rho (1, z, z^2, f^2, zf, f) dz. \quad (49)$$

## 6. Motion equations

The motion equations can be derived based on Hamilton's principle as follows

$$\int_0^t (\delta U - \delta W - \delta K) dt = 0. \quad (50)$$

### 6.1 CST

Substituting Eqs. (23), (24), (25), (27), (33) and (34) into Eq. (50) yields the FSDT motion equations as follows

$$\delta u: \frac{\partial N_{xx}}{\partial x} + \frac{\partial N_{x\theta}}{R \partial \theta} + R_x^m = I_0 \frac{\partial^2 u}{\partial t^2}, \quad (51a)$$

$$\delta v: \frac{\partial N_{x\theta}}{\partial x} + \frac{\partial N_{\theta\theta}}{R \partial \theta} + R_\theta^m = I_0 \frac{\partial^2 v}{\partial t^2}, \quad (51b)$$

$$\delta w: \frac{\partial^2 M_{xx}}{\partial x^2} + \frac{\partial^2 M_{\theta\theta}}{R^2 \partial \theta^2} + 2 \frac{\partial^2 M_{x\theta}}{R \partial x \partial \theta} - \frac{N_\theta}{R} + \frac{\partial}{\partial x} \left( N_x^f \frac{\partial w}{\partial x} \right) + \frac{\partial}{R \partial \theta} \left( N_\theta^f \frac{\partial w}{R \partial \theta} \right) + q_e + q_f + \bar{R}_z^m + M_x^m + M_\theta^m = I_0 \frac{\partial^2 w}{\partial t^2}, \quad (51c)$$

$$\delta \phi: G_x + G_\theta - G_z = 0. \quad (51d)$$

### 6.2 FSDT

Substituting Eqs. (35), (36), (25), (27), (38) and (39) into Eq. (50) yields the CST motion equations as follows

$$\delta u: \frac{\partial N_{xx}}{\partial x} + \frac{\partial N_{x\theta}}{R \partial \theta} + R_x^m = I_0 \frac{\partial^2 u}{\partial t^2} + I_1 \frac{\partial^2 \psi_x}{\partial t^2}, \quad (52a)$$

$$\delta v: \frac{\partial N_{x\theta}}{\partial x} + \frac{\partial N_{\theta\theta}}{R \partial \theta} + \frac{Q_\theta}{R} + R_\theta^m = I_0 \frac{\partial^2 v}{\partial t^2} + I_1 \frac{\partial^2 \psi_\theta}{\partial t^2}, \quad (52b)$$

$$\delta w: \frac{\partial Q_x}{\partial x} + \frac{\partial Q_\theta}{R \partial \theta} + \frac{\partial}{\partial x} \left( N_x^f \frac{\partial w}{\partial x} \right) + \frac{\partial}{R \partial \theta} \left( N_\theta^f \frac{\partial w}{R \partial \theta} \right) + q_e + q_f + R_z^m = I_0 \frac{\partial^2 w}{\partial t^2}, \quad (52c)$$

$$\delta \psi_x: \frac{\partial M_{xx}}{\partial x} + \frac{\partial M_{x\theta}}{R \partial \theta} - Q_x + M_x^m = I_1 \frac{\partial^2 u}{\partial t^2} + I_2 \frac{\partial^2 \psi_x}{\partial t^2}, \quad (52d)$$

$$\delta \psi_\theta: \frac{\partial M_{x\theta}}{\partial x} + \frac{\partial M_{\theta\theta}}{R \partial \theta} - Q_\theta + M_\theta^m = I_1 \frac{\partial^2 v}{\partial t^2} + I_2 \frac{\partial^2 \psi_\theta}{\partial t^2}, \quad (52e)$$

$$asdf \delta \phi: G_x + G_\theta - G_z = 0. \quad (52f)$$

### 6.3 SSDT

Substituting Eqs. (40), (41), (25), (27), (43) and (44) into Eq. (50) yields the CST motion equations as follows

$$\delta u: \frac{\partial N_{xx}}{\partial x} + \frac{\partial N_{x\theta}}{R \partial \theta} + R_x^m = I_0 \frac{\partial^2 u}{\partial t^2}, \quad (53a)$$

$$\delta v: \frac{\partial N_{x\theta}}{\partial x} + \frac{\partial N_{\theta\theta}}{R \partial \theta} + \frac{Q_\theta}{R} + R_\theta^m = I_0 \frac{\partial^2 v}{\partial t^2}, \quad (53b)$$

$$\delta w_b: \frac{\partial^2 M_{xx}}{\partial x^2} + \frac{\partial^2 M_{\theta\theta}}{R^2 \partial \theta^2} + 2 \frac{\partial^2 M_{x\theta}}{R \partial x \partial \theta} - \frac{N_\theta}{R} + \frac{\partial}{\partial x} \left( N_x^f \frac{\partial w_b}{\partial x} \right) + \frac{\partial}{R \partial \theta} \left( N_\theta^f \frac{\partial w_b}{R \partial \theta} \right) + q_e + q_f + R_z^m + M_x^m + M_\theta^m = I_0 \left( \frac{\partial^2 w_b}{\partial t^2} + \frac{\partial^2 w_s}{\partial t^2} \right) - (I_2 + I_4) \left( \frac{\partial^4 w_b}{\partial t^2 \partial x^2} + \frac{\partial^4 w_b}{R^2 \partial t^2 \partial \theta^2} \right), \quad (53c)$$

$$\delta w_s: \frac{\partial^2 S_{xx}}{\partial x^2} + \frac{\partial^2 S_{\theta\theta}}{R^2 \partial \theta^2} + 2 \frac{\partial^2 S_{x\theta}}{R \partial x \partial \theta} + \frac{\partial F_{xx}}{\partial x} + \frac{\partial F_{\theta\theta}}{R \partial \theta} + \frac{\partial}{\partial x} \left( N_x^f \frac{\partial w_s}{\partial x} \right) + \frac{\partial}{R \partial \theta} \left( N_\theta^f \frac{\partial w_s}{R \partial \theta} \right) \quad (53d)$$

$$\begin{aligned}
& + q_e + q_f + R_z^m + M_x^m + M_\theta^m \\
& = I_0 \left( \frac{\partial^2 w_b}{\partial t^2} + \frac{\partial^2 w_s}{\partial t^2} \right) \\
& - (I_3 + I_4) \left( \frac{\partial^4 w_s}{\partial t^2 \partial x^2} + \frac{\partial^4 w_s}{R^2 \partial t^2 \partial \theta^2} \right),
\end{aligned} \quad (53d)$$

$$\delta\phi: G_x + G_\theta - G_z = 0, \quad (53e)$$

In above relations  $N_x^f$  and  $N_\theta^f$  are combination of mechanical and electrical forces which can be expressed in dimensionless form as

$$N_x^f = N_x^M + N_x^E \rightarrow \begin{cases} N_x^M = 0, \\ N_x^E = 2e_{31}V_0, \end{cases} \quad (54a)$$

$$N_\theta^f = N_\theta^M + N_\theta^E \rightarrow \begin{cases} N_\theta^M = 0, \\ N_\theta^E = 2e_{32}V_0, \end{cases} \quad (54b)$$

However, combining Eqs. (10)-(13), (45)-(48), the motion equations may be obtained.

## 7. Solution method

DQM is used in this paper which approximates the partial derivative of a function with respect to a spatial variable at a given discrete. Hence, the  $n^{\text{th}}$ -order and  $m^{\text{th}}$ -order of partial derivative of function  $F(x, \theta)$  with respect to  $x$  and  $\theta$  respectively, can be written at the point  $(x_i, \theta_i)$ , as follows (Ghorbanpour Arani *et al.* 2015b)

$$\frac{d^n F(x_i, \theta_j)}{dx^n} = \sum_{k=1}^{N_x} A_{ik}^{(n)} F(x_k, \theta_j) \quad n = 1, \dots, N_x - 1, \quad (55)$$

$$\frac{d^m F(x_i, \theta_j)}{d\theta^m} = \sum_{l=1}^{N_\theta} B_{jl}^{(m)} F(x_i, \theta_l) \quad m = 1, \dots, N_\theta - 1, \quad (56)$$

$$\frac{d^{n+m} F(x_i, \theta_j)}{dx^n d\theta^m} = \sum_{k=1}^{N_x} \sum_{l=1}^{N_\theta} A_{ik}^{(n)} B_{jl}^{(m)} F(x_k, \theta_l), \quad (57)$$

where  $A_{ik}^{(n)}$  and  $B_{jl}^{(m)}$  are the weighting coefficients corresponding to the  $n^{\text{th}}$ -order and  $m^{\text{th}}$ -order partial derivative of  $F(x, \theta)$  with respect to  $x$  and  $\theta$  respectively, which can be written for first derivative as follows

$$A_{ij}^{(1)} = \begin{cases} \frac{M(x_i)}{(x_i - x_j)M(x_j)}, & \text{for } i \neq j, \quad i, j = 1, 2, \dots, N_x \\ -\sum_{\substack{j=1 \\ i \neq j}}^{N_x} A_{ij}^{(1)}, & \text{for } i = j, \quad i, j = 1, 2, \dots, N_x \end{cases} \quad (58a)$$

$$B_{ij}^{(1)} = \begin{cases} \frac{P(\theta_i)}{(\theta_i - \theta_j)P(\theta_j)}, & \text{for } i \neq j, \quad i, j = 1, 2, \dots, N_\theta \\ -\sum_{\substack{j=1 \\ i \neq j}}^{N_\theta} B_{ij}^{(1)}, & \text{for } i = j, \quad i, j = 1, 2, \dots, N_\theta \end{cases} \quad (58b)$$

where

$$M(x_i) = \prod_{\substack{j=1 \\ j \neq i}}^{N_x} (x_i - x_j), \quad (59a)$$

$$P(\theta_i) = \prod_{\substack{j=1 \\ j \neq i}}^{N_\theta} (\theta_i - \theta_j). \quad (59b)$$

Noted that for higher order derivative, the following formulas can be used

$$A_{ij}^{(n)} = n \left( A_{ii}^{(n-1)} A_{ij}^{(1)} - \frac{A_{ij}^{(n-1)}}{(x_i - x_j)} \right), \quad (60a)$$

$$B_{ij}^{(m)} = m \left( B_{ii}^{(m-1)} B_{ij}^{(1)} - \frac{B_{ij}^{(m-1)}}{(\theta_i - \theta_j)} \right). \quad (60b)$$

In addition,  $N_x$  and  $N_\theta$  are the number of grid points in  $x$  and  $\theta$  directions respectively, which can be obtained by Chebyshev polynomials as follows

$$x_i = \frac{L}{2} \left[ 1 - \cos \left( \frac{i-1}{N_x-1} \pi \right) \right], \quad i = 1, \dots, N_x \quad (61a)$$

$$\theta_i = \frac{2\pi}{2} \left[ 1 - \cos \left( \frac{i-1}{N_\theta-1} \pi \right) \right]. \quad i = 1, \dots, N_\theta \quad (61b)$$

However, applying DQM to motion equations yields the following coupled matrix equations

$$\begin{aligned}
[M] \begin{bmatrix} \ddot{Y}_b \\ \ddot{Y}_d \end{bmatrix} + \underbrace{\left( [C_L + C_{NL}] + (v_x) [C]^f \right)}_{[C]} \begin{bmatrix} \dot{Y}_b \\ \dot{Y}_d \end{bmatrix} \\
+ \underbrace{\left( [K_L + K_{NL}] + (v_x)^2 [K]^f \right)}_{[K]} \begin{bmatrix} Y_b \\ Y_d \end{bmatrix} = \begin{bmatrix} 0 \\ 0 \end{bmatrix},
\end{aligned} \quad (62)$$

where  $[K]$  and  $[K_{NL}]$  are the linear and nonlinear stiffness matrixes, respectively;  $[C_L]$  and  $[C_{NL}]$  are the linear and nonlinear damp matrixes, respectively;  $[C]^f$  and  $[K]^f$  are the respectively, damping and stiffness matrixes related to pulsating fluid;  $[M]$  is the mass matrix;  $\{Y\}$  is the displacement vector (i.e.,  $\{Y\} = \{u, v, w_b, w_s, \psi_x, \psi_\theta\}$ ; subscript  $b$  and  $d$  represent boundary and domain points.

For obtaining the DIR of system, the Bolotin method (Ghorbanpour Arani *et al.* 2015b) is used which, the displacement vector in the Fourier series with period  $2T$  can be expressed as follows

$$\{Y_d\} = \sum_{m=1,3,\dots}^{\infty} \left[ \{a\}_m \sin \frac{m\omega T}{2} + \{b\}_m \cos \frac{m\omega T}{2} \right]. \quad (63)$$

Substituting Eq. (63) into Eq. (62), setting the coefficients of sine and equal to zero, yields

$$\left| \left( [K] + \left( 1 \pm \alpha + \frac{\alpha^2}{2} \right) [K]^f \right) + \left( \pm [C] \frac{\omega}{2} + \left( \frac{\alpha\omega}{4} \pm \frac{\omega}{2} \right) [C]^f \right) - [M] \frac{\omega^2}{4} \right| = 0. \quad (64)$$

However, based on a direct iterative method, the variation of  $\omega$  with respect to  $\alpha$  as DIR of system can be obtained.

## 8. Numerical result

In this section, a PVDF separator modelled with cylindrical shell is considered with  $a/h = 40$  and  $h/R = 0.04$ . The mechanical and electrical properties of PVDF are listed in Table 1 (Jalili 2010).

Table 1 Mechanical and electrical properties of PVDF

PVDF	SWCNT
$C_{11} = 238.24$ (GPa)	$E = 1$ (TPa)
$C_{22} = 23.6$ (GPa)	$\nu = 0.34$
$C_{12} = 3.98$ (GPa)	$\rho = 2300$ Kg/m <sup>3</sup>
$C_{66} = 6.43$ (GPa)	
$e_{11} = -0.135$ (C/m <sup>2</sup> )	
$e_{12} = -0.145$ (C/m <sup>2</sup> )	
$\epsilon = 1.1068 \times 10^{-8}$ (F/m)	
$\rho = 1780$ Kg/m <sup>3</sup>	

Defining the dimensionless parameters as follows

$$(U, V, W_b, W_s) = \frac{(u, v, w_b, w_s)}{h}, \quad X = \frac{x}{a}, \quad Z = \frac{z}{h},$$

$$\alpha = \frac{h}{a}, \quad \beta = \frac{h}{R}, \quad \gamma = \frac{h}{R}, \quad \psi_j = \Psi_j,$$

$$Q_{11} = \frac{C_{11}}{C_{11}} - \frac{(C_{13})^2}{C_{11}C_{33}}, \quad Q_{12}^{(k)} = \frac{C_{12}}{C_{11}} - \frac{C_{13}C_{23}}{C_{11}C_{33}},$$

$$Q_{22} = \frac{C_{22}}{C_{11}} - \frac{(C_{23})^2}{C_{11}C_{33}}, \quad Q_{44} = \frac{C_{44}}{C_{11}}, \quad Q_{55} = \frac{C_{55}}{C_{11}}, \quad Q_{66} = \frac{C_{66}}{C_{11}}$$

$$\Phi = \frac{\phi}{\phi_0}, \quad V^* = \frac{V_0}{\phi_0}, \quad \phi_0 = h \sqrt{\frac{C_{11}}{\epsilon_{11}}}, \quad \epsilon_1 = \frac{\epsilon_{22}}{\epsilon_{11}}, \quad \epsilon_2 = \frac{\epsilon_{33}}{\epsilon_{11}},$$

$$K_{1W} = \frac{k_{1w}h}{C_{11}}, \quad K_{2W} = \frac{k_{2w}(h)^3}{C_{11}},$$

$$\left( E_{31}, E_{32}, E_{24}, E_{15} \right) = \left( e_{31} - e_{33} \frac{C_{13}}{C_{33}}, e_{32} - e_{33} \frac{C_{23}}{C_{33}}, e_{24}, e_{15} \right) \sqrt{\frac{C_{11}}{\epsilon_{11}}},$$

$$\Omega = \omega h \sqrt{\frac{\rho}{C_{11}}}, \quad (K_{G\xi}, K_{G\zeta}) = \frac{(k_{g\xi}, k_{g\zeta})}{C_{11}a}, \quad C_D = \frac{c_d}{\sqrt{\rho C_{11}}},$$

$$(H_X^*, H_Y^*) = \frac{(H_x, H_y)}{C_{11}}, \quad T = \frac{t}{h} \sqrt{\frac{C_{11}}{\rho}}, \quad G = \frac{g}{h} \sqrt{\frac{C_{11}}{\rho}}.$$

and clamped-clamped mechanical and free electrical boundary conditions, the dimensionless pulsation frequency is obtained and the effects of different parameters are shown.

### 8.1 Convergence of DQM

The convergence and accuracy of the DQM in evaluating the DIR for CST, FSDT and SSDT are shown in Figs. 2(a)-(c). The results are illustrated for different values of grid points. Fast rate of convergence of the methods are quite evident and it can be found that 14 and 16 grid points can yield accurate results in CST and FSDT-SSDT, respectively.

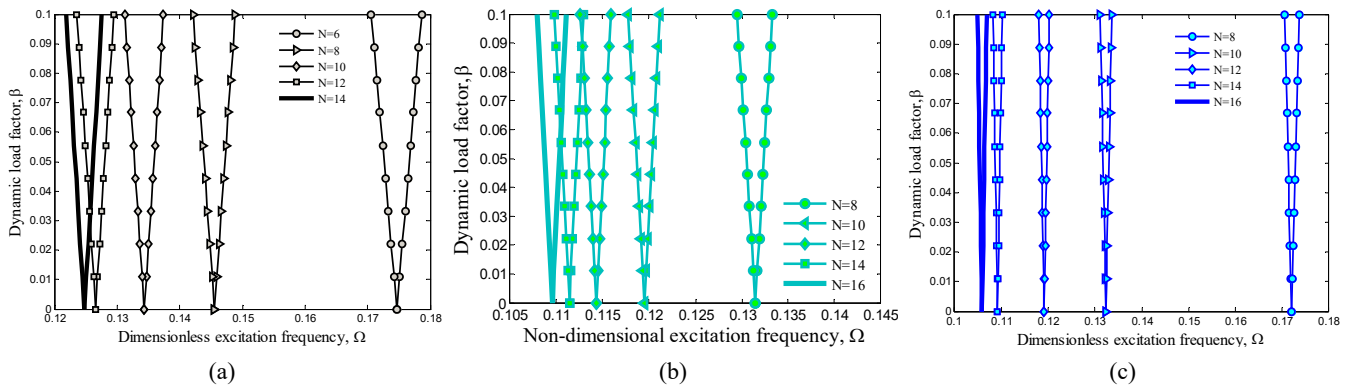


Fig. 2 Convergence and accuracy of DQM

8.2 Validation

To the best of our knowledge, dynamic stability of viscoelastic piezoelectric separators conveying pulsating fluid has not reported by researchers. However, neglecting fluid, structural damping, SWCNTs as reinforce, piezoelectric properties and elastic foundation, present results obtained by SSDT are compared with other published works for vibration analysis of cylindrical shell using 3D elasticity (Armenakas *et al.* 1969), refined higher-order shear deformation theory (RHOST) (Khalili *et al.* 2012) and parabolic shear distribution theory (PSDT) (Bhimaraddi 1984). Considering the material properties the same as (Armenakas *et al.* 1969), the first dimensionless frequency ( $\Omega = \omega h / \pi \sqrt{\rho / G}$ ) for simply supported cylindrical shell is reported in Table 2. As can be seen, present results are in a good agreement with those reported by Armenakas *et al.* (1969) and Khalili *et al.* (2012).

8.3 The effect of different parameters

In order to show the dimensionless external electric voltage ( $V^*$ ) effect on the DIR of the structure is illustrated in Fig. 3(a)-(c), respectively for CST, FSDT and SSDT. As can be seen applying negative voltage increases the dimensionless pulsation frequency and consequently shifts the DIR of system to higher frequency zone. This phenomenon is vice versa for positive voltage. This is due to the fact that the imposed negative and positive voltages generate the axial tensile and compressive forces in the separator, respectively. However, external voltage is an effective parameter for controlling the DIR of system.

In realizing the influence of SWCNT volume percent, the DIR of viscoelastic structure is shown in Figs. 4(a)-(c), respectively for CST, FSDT and SSDT. It can be found that with neglecting SWCNT as reinforcer, the resonance region will be happen in lower frequencies with respect to

Table 2 Comparison of first dimensionless frequency for simply supported cylindrical shell

L/R		h/R			
		0.06	0.10	0.12	0.18
2	Armenakas <i>et al.</i> (1969)	0.01853	0.03100	0.03730	0.05652
	Khalili <i>et al.</i> (2012)	0.01853	0.03100	0.03729	0.05650
	Bhimaraddi (1984)	0.01853	0.03100	0.03730	0.05653
	SSDT, Present	0.01853	0.03100	0.03730	0.05654
1	Armenakas <i>et al.</i> (1969)	0.02781	0.04784	0.05853	0.09402
	Khalili <i>et al.</i> (2012)	0.02780	0.04779	0.05847	0.09385
	Bhimaraddi (1984)	0.02781	0.04785	0.05856	0.09409
	SSDT, Present	0.02781	0.04785	0.05855	0.09405
0.5	Armenakas <i>et al.</i> (1969)	0.03691	0.07618	0.10057	0.18894
	Khalili <i>et al.</i> (2012)	0.03688	0.07607	0.10042	0.18864
	Bhimaraddi (1984)	0.03692	0.07615	0.10047	0.18832
	SSDT, Present	0.03694	0.07620	0.10056	0.18898
0.25	Armenakas <i>et al.</i> (1969)	0.08639	0.20529	0.27491	0.50338
	Khalili <i>et al.</i> (2012)	0.08635	0.20525	0.27493	0.50406
	Bhimaraddi (1984)	0.08639	0.20478	0.27286	0.49818
	SSDT, Present	0.08642	0.20533	0.27499	0.50345

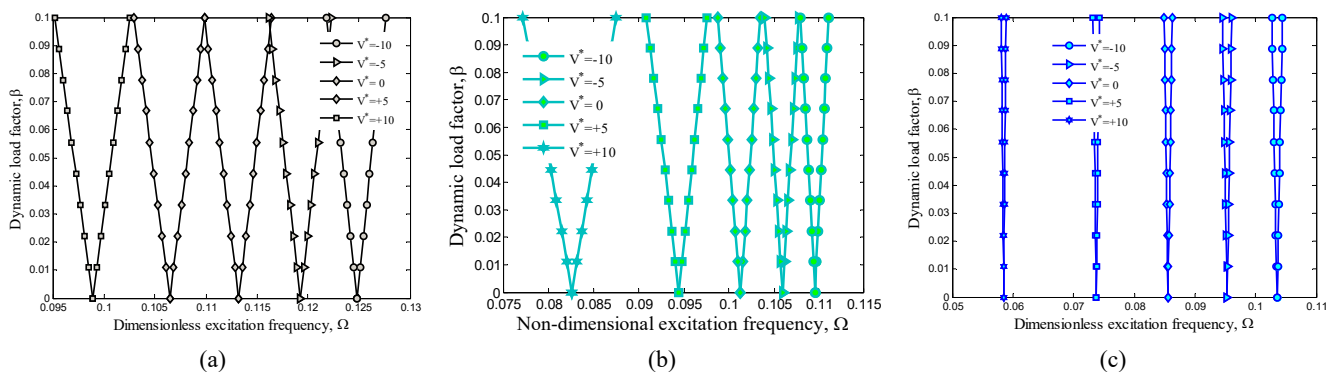


Fig. 3 The effects of external electric voltage on the dynamic stability of separator

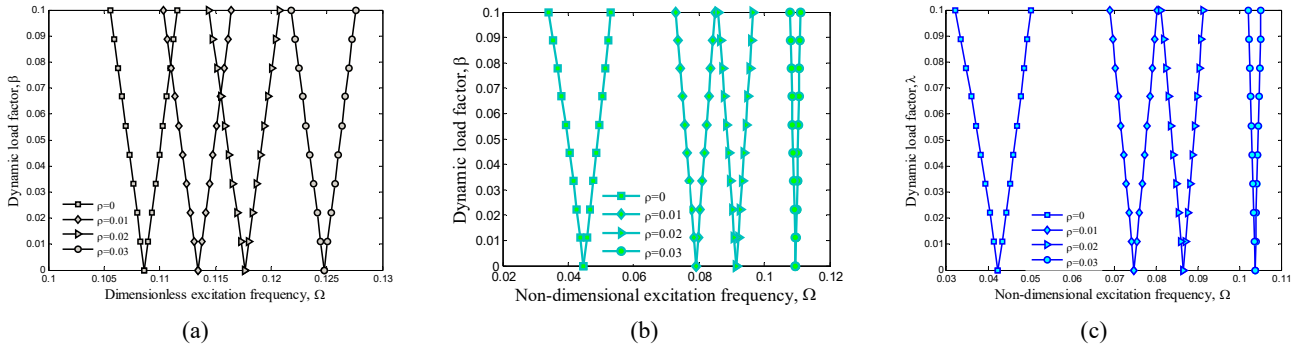


Fig. 4 The effects of SWCNT as reinforcer on the dynamic stability of separator

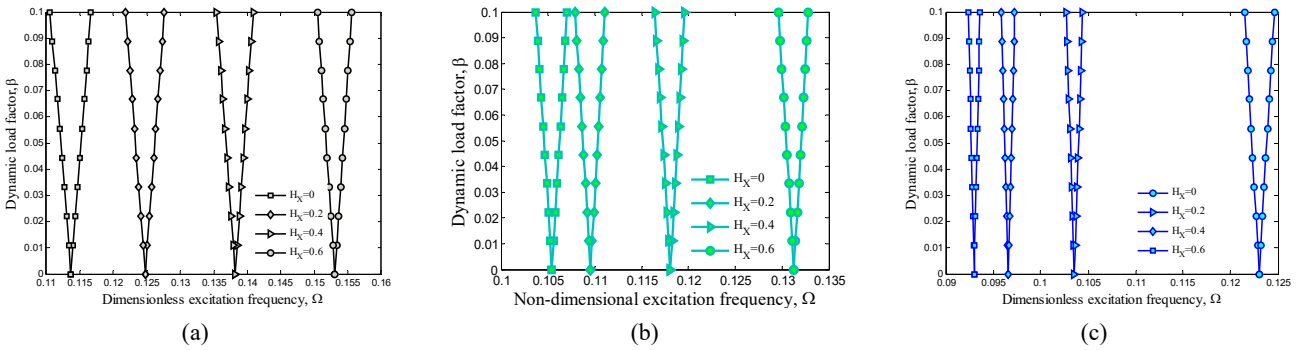


Fig. 5 The effects of magnetic field on the dynamic stability of separator

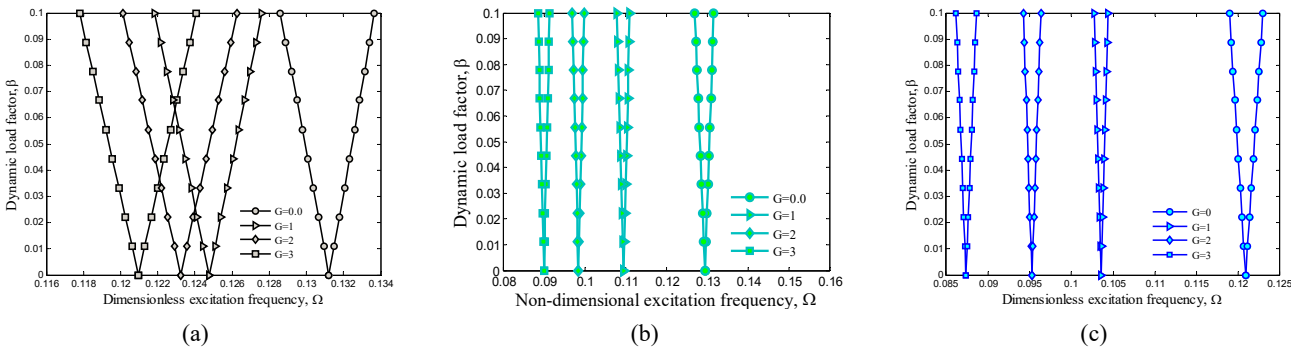


Fig. 6 The effects of structural damping on the dynamic stability of separator

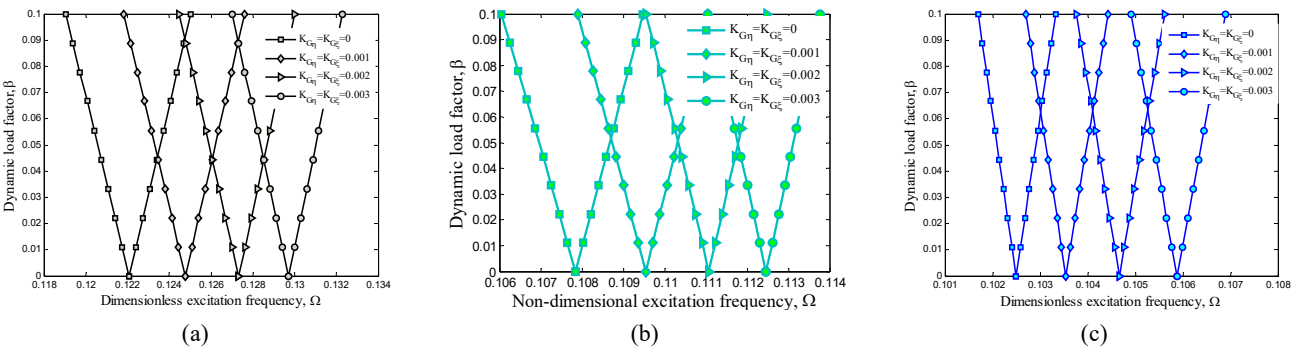


Fig. 7 The effects of shear constant of viscoelastic medium on the dynamic stability of separator

Figs. 6(a)-(c) demonstrates the DIR of structure for CST, FSDT and SSDT, respectively for different structural damping parameters. It can be found that the DIR and

natural frequency of viscoelastic separator are lower than those of non-visco one. This remarkable difference shows that considering the nature of separator as viscoelastic can

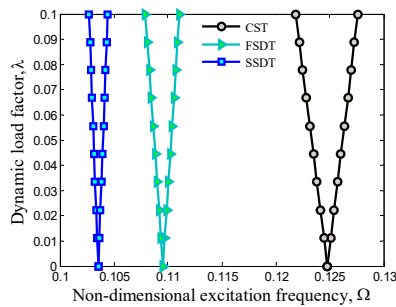


Fig. 8 Comparison of DIR obtained by CST, FSDT and SSDT

yields the accurate results with respect to non-visco ones. The reason is that assuming viscoelastic structure means induce of damping force which results in more absorption of energy by the system.

Figs. 7(a)-(c) illustrates the influence of shear constant of elastic medium on the DIR of structure respectively for CST, FSDT and SSDT. As can be seen, the higher the shear constants for elastic medium, the higher are the DIR and dimensionless resonant frequency. This is perhaps because increasing Pasternak coefficient increases the structure stiffness. Final figure is related to comparison of DIR and pulsation frequency for three applied theories namely as CST, FSDT and SSDT. It can be seen that the DIR obtained by SSDT is happen in lower pulsation frequency with respect to two other theories. It is perhaps due to the fact that the flexibility of structure modeled by SSDT is lower than other theories. Furthermore, the displacement field in SSDT is close to the deflection of structure and it can be another reason for more accuracy of this theory. It can be also found that the results calculated by CST are much overestimated with respect to FSDT and SSDT.

## 9. Conclusions

Based on CST, FSDT and SSDT, a comparative study on the dynamic stability of piezo-visco-separators conveying pulsating fluid was presented in this work. In order to consider the nanotechnology effects on the dynamic stability of separator, it was reinforced with SWCNT. The separator was subjected to 3D electric and 2D magnetic fields and was surrounded by nonlinear orthotropic visco Pasternak foundation. Using DQM in conjunction with Bolotin's method, the derived motion equations were discretized and solved to obtain the DIR and resonance frequency of system. The effects of different parameters such as external voltage, magnetic field, visco-Pasternak foundation, structural damping and volume percent of SWCNTs were shown on the dynamic instability of structure. The most important findings of this paper are:

- The DIR obtained by SSDT was happen in lower pulsation frequency with respect to two other theories.
- Applying negative voltage increases the dimensionless pulsation frequency and consequently shifts the DIR of system to higher frequency zone.

- With increasing magnetic field intensity, the pulsation frequency increases and the DIR shifts to right.
- With neglecting SWCNT as reinforcer, the resonance region will be happen in lower frequencies with respect to considering SWCNT.
- The DIR and natural frequency of viscoelastic separator were lower than those of non-visco one. The results of this study were validated by other works.

Finally, it was hoped that the results of this paper would be beneficial for the design of separators used in oil and gas industries.

## Acknowledgments

I should thank from Pars Oil and Gas Co. for having sponsored this project.

## References

- Alibeigloo, A. and Kani, A.M. (2010), "3D free vibration analysis of laminated cylindrical shell integrated piezoelectric layers using the differential quadrature method", *Appl. Math. Model.*, **34**(12), 4123-4137.
- Amabili, M. (2008), *Nonlinear Vibrations and Stability of Shells and Plates*, Cambridge University Press, New York, NY, USA.
- Amabili, M. (2011), "Nonlinear vibrations of laminated circular cylindrical shells: Comparison of different shell theories", *Compos. Struct.*, **94**(1), 207-220.
- Armenakas, A.E., Gazis, D.C. and Herrmann, G. (1969), *Free vibrations of circular cylindrical shells*, Pergamon Press, Oxford, UK.
- Bhimaraddi, A. (1984), "A higher order theory for free vibration analysis of circular cylindrical shells", *Int. J. Solids Struct.*, **20**(7), 623-630.
- De Bellis, M.L., Ruta, G.C. and Elishakoff, I. (2010), "Influence of a Wiegardt foundation on the dynamic stability of a fluid conveying pipe", *Arch. Appl. Mech.*, **80**(7), 785-801.
- Duc, N.D. and Than, P.T. (2015), "Nonlinear dynamic response and vibration of shear deformable imperfect eccentrically stiffened S-FGM circular cylindrical shells surrounded on elastic foundations", *Aero Sci. Tech.*, **40**, 115-127.
- Formica, G., Lacarbonara, W. and Alessi, R. (2010), "Vibrations of carbon nanotube-reinforced composites", *J. Sound Vib.*, **329**(10), 1875-1889.
- Ghorbanpour Arani, A., Golabi, S., Loghman, A. and Daneshi, H. (2007), "Investigating elastic stability of cylindrical shell with an elastic core under axial compression by energy method", *J. Mech. Sci. Tech.*, **21**(7), 693-698.
- Ghorbanpour Arani, A., Mohammadimehr, M., Arefmanesh, A. and Ghasemi, A. (2010), "Transverse vibration of short carbon nanotubes using cylindrical shell and beam models", *Proceed Inst. Mech. Eng., Part C, J. Mech. Eng. Sci.*, **224**(3), 745-756.
- Ghorbanpour Arani, A., Maghamikia, Sh., Mohammadimehr, M. and Arefmanesh, A. (2011a), "Buckling analysis of laminated composite rectangular plates reinforced by SWCNTs using analytical and finite element methods", *J. Mech. Sci. Tech.*, **25**(3), 809-820.
- Ghorbanpour Arani, A., Loghman, A., Abdollahitaheri, A. and Atabakhshian, V. (2011b), "Electrothermomechanical behavior of a radially polarized rotating functionally graded piezoelectric cylinder", *J. Mech. Mat. Struct.*, **6**(6), 869-882.

- Ghorbanpour Arani, A., Shajari, A.R., Amir, S. and Loghman, A. (2012), "Electro-thermo-mechanical nonlinear nonlocal vibration and instability of embedded micro-tube reinforced by BNNT, conveying fluid", *Physica E*, **45**(3), 109-121.
- Ghorbanpour Arani, A., Kolahchi, R. and Khoddami Maraghi, Z. (2013a), "Nonlinear vibration and instability of embedded double-walled boron nitride nanotubes based on nonlocal cylindrical shell theory", *Appl. Math. Model.*, **37**(14), 7685-7707.
- Ghorbanpour Arani, A., Haghshenas, A., Amir, S., Mozdianfar, M.R. and Latifi, M. (2013b), "Electro-thermo-mechanical response of thick-walled piezoelectric cylinder reinforced by boron-nitride nanotubes", *Strength Mat.*, **45**(1), 102-115.
- Ghorbanpour Arani, A., Haghparast, E., Khoddami Maraghi, Z. and Amir, S. (2015a), "Static stress analysis of carbon nano-tube reinforced composite (CNTRC), cylinder under non-axisymmetric thermo-mechanical loads and uniform electromagnetic fields", *Compos. Part B, Eng.*, **68**, 136-145.
- Ghorbanpour Arani, A., Kolahchi, R. and Zarei, M.Sh. (2015b), "Visco-surface-nonlocal piezoelectricity effects on nonlinear dynamic stability of graphene sheets integrated with ZnO sensors and actuators using refined zigzag theory", *Compos. Struct.*, **132**, 506-526.
- Ghorbanpour Arani, A., Abdollahian, M. and Kolahchi, R. (2015c), "Nonlinear vibration of embedded smart composite microtube conveying fluid based on modified couple stress theory", *Polym. Compos.*, **36**(7), 1314-1324.
- Jalili, N. (2010), *Piezoelectric-Based Vibration Control from Macro to Micro/Nano Scale Systems*, Springer Science, New York, NY, USA.
- Kadoli, R. and Ganesan, N. (2003), "Free vibration and buckling analysis of composite cylindrical shells conveying hot fluid", *Compos. Struct.*, **60**(1), 19-32.
- Khalili, S.M.R., Davar, A. and Malekzadeh Fard, K. (2012), "Free vibration analysis of homogeneous isotropic circular cylindrical shells based on a new three-dimensional refined higher-order theory", *Int. J. Mech. Sci.*, **56**(1), 1-25.
- Kumar, A., Chakrabarti, A. and Bhargava, P. (2013a), "Finite element analysis of laminated composite and sandwich shells using higher order zigzag theory", *Compos. Struct.*, **106**, 270-281.
- Kumar, A., Chakrabarti, A. and Bhargava, P. (2013b), "Vibration of laminated composites and sandwich shells based on higher order zigzag theory", *Eng. Struct.*, **56**, 880-888.
- Kumar, A., Chakrabarti, A. and Bhargava, P. (2013c), "Vibration of laminated composite skew hypar shells using higher order theory", *Thin-Wall. Struct.*, **63**, 82-90.
- Kumar, A., Chakrabarti, A. and Bhargava, P. (2014), "Accurate dynamic response of laminated composites and sandwich shells using higher order zigzag theory", *Thin-Wall. Struct.*, **77**, 174-186.
- Kumar, A., Chakrabarti, A. and Bhargava, P. (2015), "Vibration analysis of laminated composite skew cylindrical shells using higher order shear deformation theory", *J. Vib. Control*, **21**(4), 725-735.
- Lei, Z.X., Zhang, L.W., Liew, K.M. and Yu, J.L. (2014), "Dynamic stability analysis of carbon nanotube-reinforced functionally graded cylindrical panels using the element-free kp-Ritz method", *Compos. Struct.*, **113**, 328-338.
- Liew, K.M., Lei, Z.X., Yu, J.L. and Zhang, L.W. (2014), "Postbuckling of carbon nanotube-reinforced functionally graded cylindrical panels under axial compression using a meshless approach", *Comput. Methods Appl. Mech. Engrg.*, **268**, 1-17.
- Liu, Ch., Ke, L.L., Wang, Y.Sh., Yang, J. and Kitipornchai, S. (2013), "Thermo-electro-mechanical vibration of piezoelectric nanoplates based on the nonlocal theory", *Compos. Struct.*, **106**, 167-174.
- Madani, H., Hosseini, H. and Shokravi, M. (2016), "Differential cubature method for vibration analysis of embedded FG-CNT-reinforced piezoelectric cylindrical shells subjected to uniform and non-uniform temperature distributions", *Steel Compos. Struct., Int. J.*, **22**(4), 889-913.
- Mahdi, M. and Katebi, H. (2015), "Numerical modeling of uplift resistance of buried pipelines in sand, reinforced with geogrid and innovative grid-anchor system", *Geomech. Eng., Int. J.*, **9**(6), 757-774.
- Mantari, J.L. and Guedes Soares, C. (2014), "Optimized sinusoidal higher order shear deformation theory for the analysis of functionally graded plates and shells", *Compos. Part B*, **56**, 126-136.
- Mohammadi, F. and Sedaghati, R. (2012), "Vibration analysis and design optimization of viscoelastic sandwich cylindrical shell", *J. Sound Vib.*, **331**(12), 2729-2752.
- Patel, S.N., Datta, P.K. and Sheikh, A.H. (2006), "Buckling and dynamic instability analysis of stiffened shell panels", *Thin-Wall. Struct.*, **44**(3), 321-333.
- Rabani Bidgoli, M., Karimi, M.S. and Ghorbanpour Arani, A. (2016), "Viscous fluid induced vibration and instability of FG-CNT-reinforced cylindrical shells integrated with piezoelectric layers", *Steel Compos. Struct., Int. J.*, **19**(3), 713-733.
- Seo, Y.S., Jeong, W.B., Yoo, W.S. and Jeong, H.K. (2015), "Frequency response analysis of cylindrical shells conveying fluid using finite element method", *J. Mech. Sci. Tech.*, **19**(2), 625-633.
- Sheng, G.G. and Wang, X. (2010), "Thermoelastic vibration and buckling analysis of functionally graded piezoelectric cylindrical shells", *Appl. Math. Model.*, **34**(9), 2630-2643.
- Srivastava, A. and Sivakumar Babu, G.L. (2011), "Deflection and buckling of buried flexible pipe-soil system in a spatially variable soil profile", *Geomech. Eng., Int. J.*, **3**(3), 169-188.
- Thai, H.T. and Vo, T.P. (2013), "A new sinusoidal shear deformation theory for bending, buckling, and vibration of functionally graded plates", *Appl. Math. Model.*, **37**(5), 3269-3281.
- Tzou, H.S. and Gadre, M. (1989), "Theoretical analysis of a multi-layered thin shell coupled with piezoelectric shell actuators for distributed vibration controls", *J. Sound Vib.*, **132**(3), 433-450.
- Uematsu, Y., Tsujiguchi, N. and Yamada, M. (2001), "Mechanism of ovaling vibrations of cylindrical shells in cross flow", *Wind Struct., Int. J.*, **4**(2), 85-100.
- Wang, L. (2009), "A further study on the non-linear dynamics of simply supported pipes conveying pulsating fluid", *Int. J. Non-Linear Mech.*, **44**(1), 115-121.
- Yang, Ch., Jin, G., Liu, Zh., Wang, X. and Miao, X. (2015), "Vibration and damping analysis of thick sandwich cylindrical shells with a viscoelastic core under arbitrary boundary conditions", *Int. J. Mech. Sci.*, **92**, 162-177.
- Zhang, J.F., Ge, Y.J. and Zhao, L. (2013), "Influence of latitude wind pressure distribution on the responses of hyperboloidal cooling tower shell", *Wind Struct., Int. J.*, **16**(6), 579-601.
- Zhang, L.W., Lei, Z.X., Liew, K.M. and Yu, J.L. (2014a), "Large deflection geometrically nonlinear analysis of carbon nanotube-reinforced functionally graded cylindrical panels", *Comput. Methods Appl. Mech. Engrg.*, **273**, 1-18.
- Zhang, L.W., Lei, Z.X., Liew, K.M. and Yu, J.L. (2014b), "Static and dynamic of carbon nanotube reinforced functionally graded cylindrical panels", *Compos. Struct.*, **111**, 205-212.